Distributed cerebellar plasticity implements multiple-scale memory components of vestibular-ocular reflex in real-robots

Claudia Casellato, Alberto Antonietti, Jesus A. Garrido, Alessandra Pedrocchi, Egidio D'Angelo

***Abstract* — The cerebellum plays a crucial role in motor learning and it acts as a predictive controller. A biological inspired cerebellar model with distributed plasticity has been embedded into a real-time controller of a neurorobot. A cerebellum-driven task has been designed: the vestibular-ocular reflex (VOR), which produces eye movements stabilizing images on the retina during head movement. The cerebellar controller drives eye compensation, by providing joint torque based on network output activity.**

We compared a cerebellar controller with only the cortical plasticity and a cerebellar controller with also the plasticity mechanisms at deep nuclei, in VOR multiple sessions. The results were interpreted using a two state multi-rate model integrating two learning processes with different sensitivities to error and different retention strengths.

The cerebellar model showed effective learning along task repetitions, allowing a fine timing and gain adaptation based on the head stimulus. The multisite plasticity proved superior to single-site plasticity in generating human-like VOR acquisition, extinction and consolidation especially in complex tasks like gain-up and multi-session VOR.

I. INTRODUCTION

The cerebellum plays a crucial role in motor learning, from associative conditioning of discrete behavioral responses to on-line adaptation in voluntary and reflex movement control [1, 2].

In order to learn and store information about body-environment dynamics in internal models of movement so as to act as a predictive controller, the cerebellum is thought to employ long-term synaptic plasticity (Long-term Depression (LTD) and Long-Term Potentiation (LTP)). The plasticity at the Parallel Fibers/Purkinje Cells (PF-PC) synapses has classically been assumed to subserve this function [3]

In order to assess the role of cerebellar plasticity in learning, several cerebellar model were developed and tested in the context of various sensorimotor tasks. Simplified analog models in which learning occurred as long-term synaptic plasticity at the PF-PC synapses only, under instructive control by climbing fibers, were tested in computational simulations of classical condition and other tasks [4, 5, 6]. In order to stress the learning robustness into noisy environments, the system was embodied, i.e. the cerebellar model drove in real-time the motor learning of real robots performing collision avoidance and eye movement tasks [7, 8].

However, the model needs to be continuously enriched with cutting-edge neurophysiological knowledge. In particular, the PF-PC plasticity alone cannot account for the broad dynamic ranges and multiple time scales of cerebellar adaptation. Hence, very recently [9], beside the PF-PC cortical plastic, a cerebellum model was endowed with biological plausible plastic mechanisms at two synaptic sites of the deep cerebellar nuclei: Mossy Fibers/DCN (MF-DCN) and PC-DCN [10, 11]. The model was tested in a computational simulation of a tracking task; the cerebellar model learnt to improve the motor commands computed by a crude inverse dynamic model, successfully dealing with a varying payload at the arm end-effector.

In this work, as for the single-plasticity models, we aim at stressing the enriched cerebellar model into an embodied system, challenging it in cerebellar-mediated paradigms taken from human functional neurophysiology. Thus, we have embedded the cerebellum model into a real robotic platform performing a vestibular-ocular reflex (VOR) protocol with multiple consecutive sessions of acquisition and extinction. The VOR produces eye movements which stabilize images on the retina during head movement. The VOR tuning is ascribed mainly to the cerebellar flocculus. as indicated by lesion, pharmacological inactivation and genetic disruption studies [12].

In particular, by comparing the distributed plasticity model with a simpler one implementing only the PF-PC learning rule, we show the roles of the multiple plasticity mechanisms in real robotic sensorimotor tasks. We have interpreted the data by applying a two-state model with two learning rates [13]. Indeed, the hypothesis is that the cerebellum learns on two different time-scales, so that the cerebellar cortex operates as a fast learning module while deeper structures, like the Deep Cerebellar Nuclei, operate as a slow learning module and are responsible for a skill consolidation into persistent memory [13, 14, 15].

II. METHODS

A. Cerebellum model [9]

* This work was supported by grants of European Union: (CEREBNET FP7-ITN238686, REALNET FP7-ICT270434, Human Brain Project (HBP-604102)

C. Casellato, A. Antonietti and A. Pedrocchi are with the NeuroEngineering And medical Robotics Laboratory, Dept. Electronics, Information and Bioengineering, Politecnico di Milano, P.zza L. Da Vinci 32, 20133, Milano, Italy (telephone: +39-02-23999029 e-mail: claudia.casellato@polimi.it).

J. Garrido and E. D'Angelo are with the Brain Connectivity Center, IRCCS Istituto Neurologico Nazionale C. Mondino, Via Mondino 2, Pavia, I-27100, Italy and Dept. Brain and Behavioral Sciences, University of Pavia, Via Forlanini 6, Pavia, I-27100, Italy (e-mail: egidiougo.dangelo@unipv.it)

As input, the GRanular layer (GR) circuit is capable of generating not-recurrent time-evolving states, repeated in each trial.

The Purkinje cells, receiving error from Climbing Fibers and state information from GR, works as a state-error correlator (1). The DCN cells integrate the excitatory activity coming from MFs and the inhibitory activity coming from PCs (2). The weights of these two connections evolve as the learning rules in (3) and (4). The model is schematized in Fig 1.A.

$$\Delta W_{PF_j\text{-}PC_i}(t)=\begin{cases}\frac{LTP_{MAX}}{(\varepsilon_i+1)^{\alpha}}-LTD_{MAX}\cdot\varepsilon_i(t) & if\ PF_j\ is\ active\ at\ t\\ 0 & otherwise\end{cases} \quad (1)$$

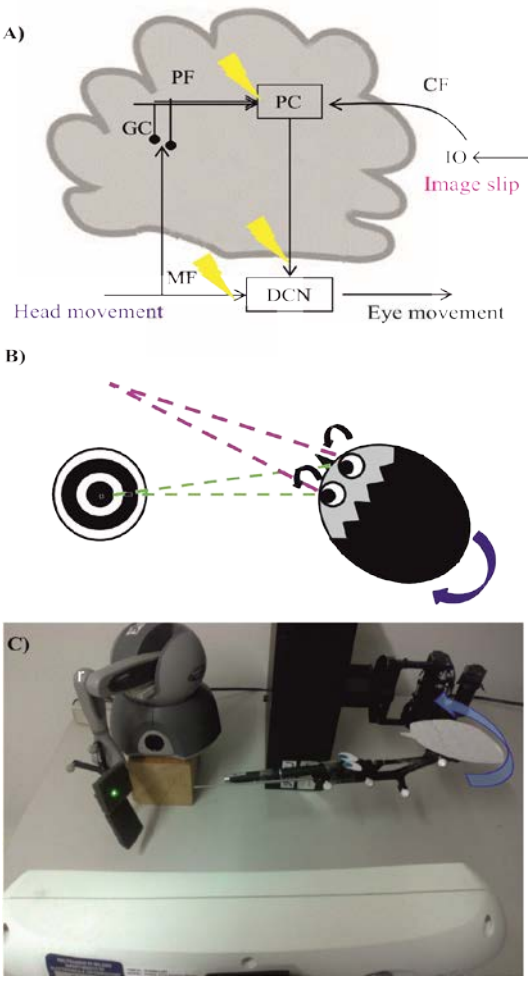

Figure 1. *Cerebellar model and set-up*

(A): cerebellar model with VOR-specific input and output signals (modified from [11]). The yellow arrows represent the plasticity sites. (B): human-like VOR task. (C): the VOR is reproduced into the robotic platform by using the second joint of the robotic arm as the head (imposed rotation) and the third joint (determining the orientation of the second link, on which the green laser is placed) as the eye. The disalignment between the gaze direction (i.e. second link orientation) and the environmental target to be looked at) is computed through geometric equations from the optical tracker recording. The image slip is fed into the Climbing Fibers pathway, head vestibular stimulus represents the system time-state, not-recurrently decoded by the GR layer; the DCN modulate the eye compensation motion.

Where $\Delta W_{PF_j\text{--}PC_i}$ is the weight change between the j^{th} PF and the i^{th} PC associated with the agonist muscle (i=1) or with the antagonist muscle (i=2), $\varepsilon_i(t)$ is the current activity coming from the associated i^{th} CF (which represents the normalized gaze error), LTP_{MAX} (=0.01) and LTD_{MAX} (=0.04) are the maximum LTP/LTD values and α is the LTP decaying factor (set at 1000 in order to allow a fast decrease of LTP and prevent early plasticity saturation).

$$DCN_i(t)=W_{MF\text{-}DCN_i}-Pur_i(t)\cdot W_{PC_i\text{-}DCN_i},\ i=1,2 \quad (2)$$

Where DCN_i represents the firing rate of the DCN cell associated with the agonist (i=1) or antagonist (i=2) muscles, $Pur_i(t)$ is the current activity coming from the associated PCs, $W_{MF\text{-}DCN_i}$ is the synaptic strength of the MF-DCN connection at the i^{th} muscle, and $W_{PC_i\text{-}DCN_i}$ is the synaptic strength of the PC-DCN connections at the i^{th} muscle.

$$\Delta W_{MF\text{-}DCN_i}(t)=\frac{LTP_{MAX}}{(Pur_i(t)+1)^{\alpha}}-LTD_{MAX}\cdot Pur_i(t),\ i=1,2 \quad (3)$$

Where $\Delta W_{MF\text{-}DCN_i}$ represents the weight change between the active MF and the target DCN associated with the i^{th} muscle, LTP_{MAX} (=$3\cdot10^{-6}$) and LTD_{MAX} (=$5\cdot10^{-8}$) are the maximum LTP/LTD values and α is the LTP decaying factor (=1000).

$$\Delta W_{PC_i\text{-}DCN_i}(t)=LTP_{MAX}\cdot Pur_i(t)^{\alpha}\cdot\left(1-\frac{1}{(DCN_i(t)+1)^{\alpha}}\right)+$$
$$-LTD_{MAX}\cdot\left(1-Pur_i(t)\right),\ i=1,2 \quad (4)$$

Where $\Delta W_{PC_i\text{-}DCN_i}$ is the synaptic weight adjustment at the PC-DCN connection reaching the DCN cell associated with the i^{th} muscle, $Pur_i(t)$ is the current activity coming from the associated PCs, $DCN_i(t)$ is the current DCN firing rate, LTP_{MAX} (=$2\cdot10^{-6}$) and LTD_{MAX} (=$2\cdot10^{-6}$) are the maximum LTP/LTD values and α is the LTP decaying factor (=1000).

B. Protocol

VOR produces eye motion compensating for head rotations in order to stabilize the visual target (Fig 1.B). The VOR learning is based on the temporal association of the two stimuli, head turn and motion of retinal image, i.e. the system learns that one stimulus will be followed by another stimulus and a consequent predictive compensatory response is gradually produced and accurately tuned [16, 17]. In real robot, the VOR protocol was reproduced by using the 2nd joint as the head, on which a desired joint displacement was imposed, and the 3rd joint as the eye motion driven only by the cerebellar module. The set-up was arranged so that the two involved joints (2nd and 3rd) moved on a horizontal plane (Fig 1.C). The visual error, thanks to the tracking system, was computed as the disalignment angle between the actual

gaze, i.e. the orientation of the second link of the robot, and the desired one aligned with the fixed object to be looked at. It was sent on the IOs corresponding to the actual error sign. The DCN activity was proportionally translated into a net torque on the 3rd joint, positive or negative depending on the error sign at each time sample [18].

The first tested protocol consisted of a sequence of 100 repetitions where a head turn of 28° in 2 seconds was imposed , followed by 100 repetitions with a head turn increased to 43°, thus requiring a VOR gain-up, and finally back to head turn of 28° in 2 seconds for 100 trials. The Root Mean Square (RMS) of gaze error was computed.

Then, a second test was carried out, made up of two VOR sessions (*session1* and *session2*) . Each VOR session consisted of 200 trials: 100 of acquisition (head rotation of 28° in 2 seconds) directly followed by 130 trials of extinction (head turn null), then a phase of 100 trials of re-acquisition (head rotation of 28° in 2 seconds) starts. Finally, a second phase of 70 trials of extinction takes place. Both tests were performed embedding the cerebellum model with one plasticity (PF-PC) and embedding the model with the three plasticity sites.

C. Set-up

The main robot was a Phantom Premium 1.0 (SensAble™), with 3 DoFs, each equipped with digital encoders and controllable by torque commands. It was integrated with an optical tracking system, a VICRA-Polaris (NDI™), acquiring marker-tools at 20 Hz. The controller, ad-hoc developed in C++, exploited the low-level access provided by the Haptic Device Application Programming Interface, sending the torque signals to the joints by servo loops (HDCALLBACKS) executed in high-priority threads at 1 kHz. For the tracking device, the low-level libraries from Image-Guided Surgery Toolkit (http://www.igstk.org/), based on Request-Observer-patterns, were used to acquire the visual information. The cerebellar adaptive module was embedded into the C++ controller.

D. The two-state model of learning

The VOR kinetics were modeled by the two state multi-rate model [19]. The net adaptation (y) was made up of the sum of two processes, fast and slow. The fast process (x_f) responded strongly to large errors but had poor retention, while the slow process (x_s) responded weakly to small errors but retained information well.

$$\boldsymbol{x}(n+\Delta n) = \boldsymbol{A}\cdot\boldsymbol{x}(n)+\boldsymbol{B}\cdot e(n)$$

$$y(n)=\boldsymbol{C}\cdot\boldsymbol{x}(n)+\boldsymbol{D}\cdot e(n)$$

$$\boldsymbol{A}=\begin{bmatrix}A_s & 0\\ 0 & A_f\end{bmatrix};\ \boldsymbol{B}=\begin{bmatrix}B_s\\ B_f\end{bmatrix};\ \boldsymbol{C}=[1\quad 1];\ \boldsymbol{D}=0$$

Where the $\boldsymbol{x}$ vector was composed by the two state vectors

$$(x_s, x_f):\ \boldsymbol{x}(n)=\begin{bmatrix}x_s(n)\\ x_f(n)\end{bmatrix}$$

B_f and B_s were the learning rates ($B_f > B_s$), A_f and A_s were the retention factors ($A_f < A_s$), n was the trial and Δn was the discrete trial increment. The motor output, i.e. the net adaptation, corresponds to the RMS of the cerebellar output within each trial. The error *e(n)* was the difference between the net adaptation *y(n)* and the "optimal" state *f(n)* dependent from the task phase (*e(n) =y(n)- f(n)*). For the acquisition phases, *f(n)* was quantified as the maximum cerebellar output reached by the network (in the plateau when the error was stabilized at minimum value). For the extinction phases, *f(n)* was quantified as zero, since no eye compensation driven by cerebellum was required. The free parameters A_s, A_f, B_s and B_f were initialized to values reported for force-field experiments:

$$\boldsymbol{A}=\begin{bmatrix}0.99 & 0\\ 0 & 0.75\end{bmatrix};\ \boldsymbol{B}=\begin{bmatrix}0.02\\ 0.3\end{bmatrix}$$

The model was applied to all VOR sessions of the second test. The two processes were initialized to zero level, corresponding to a naïve behavior. By an iterative prediction-error minimization method, the free parameters of the model were adjusted to optimize the fit with input-output coming from experimental data, i.e. the cerebellar output provided to neurorobot as output and its difference with respect to the "ideal" torque level required depending on the head stimulus (acquisition level or extinction level). The goodness-of-fit was evaluated by computing the coefficient of determination (R-square) value from actual data and model data in terms of eye compensation torque (cerebellum output).

III. Results

In these experiments we have investigated the role of multiple cerebellar plasticity sites, by testing learning during a gain-up VOR protocol and during a two-session VOR protocol, performed by a real robot. All tested acquisition phases showed that at beginning of learning, the RMS gaze error was up to 12°. During learning, the cerebellar controller tuned eye motion in order to continuously compensate head rotation. At the end of training the gaze RMS error was reduced to less than 1°. This behavior was comparable with neurophysiological studies focused on visual-vestibular training where an image slip around 0.2° was achieved [20].

The incomplete zeroing of the gaze error is due to the not repeatability in time and space across trials for uncertainty in the motion and sensory recordings of the real low friction robot used in the tests.

The gain-up VOR protocol highlighted the crucial role of multiple DCN plastic sites for implementing an adaptable gain control facing varying operative ranges (Fig. 2). The gain-up VOR adaptation could be performed only by the 3-

plasticity cerebellar controller. The 1-plasticity controller could not tune the gain, so that no adaptation was possible when PCs were already silent before the gain-up test.

The multiple-session VOR protocol shed light on the

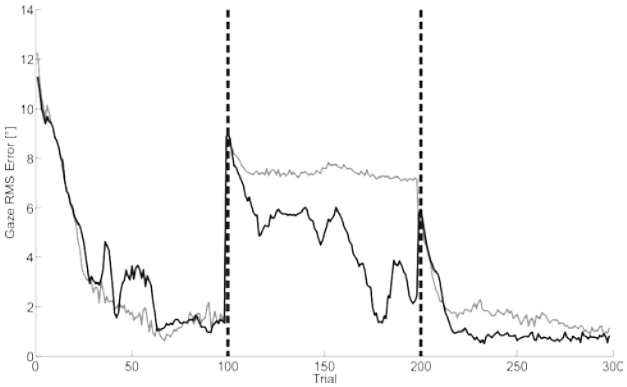

Figure 2. *VOR gain-up*

The RMS gaze error along trials is reported; in grey when the eye motion was controlled by the 1-plasticity cerebellar model, in black by the 3-plasticity cerebellar model. The vertical dashed lines separate the three sequences with different head rotation: 28°, 43° (gain-up condition) and 28° in 2 seconds.

memory factor. The two cerebellar controllers behaved similarly during a single VOR session (*session 1*), with comparable acquisition rates, steady late acquisition, and similar extinction rate. However, when the system was re-tested for the same task (*session2*), the 3-plasticity controller demonstrated a faster re-acquisition rate. Somehow, it exploited previous learned skill (Fig. 3.A): indeed, the extinction phase of *session1* did not reset all the plastic changes achieved in the acquisition training. The synaptic changes are depicted in Fig 3.B.

In order to model the 3-plasticity module behavior, the multi-rate model of learning has been applied on the multiple-session protocol (Fig. 3.C). The optimization procedure of the parameters yielded:

$$\boldsymbol{A}=\begin{bmatrix}1 & 0\\ 0 & 0.9\end{bmatrix};\ \boldsymbol{B}=\begin{bmatrix}0.03\\ 0.07\end{bmatrix}$$

Eye motion generation in the first trials was driven mainly by the fast process; then, as acquisition progressed, learning was taken over by the slow process. Finally, extinction was largely driven by the fast process. The slow process was not completely reset during extinction; thus, the starting point of the re-acquisition was slightly different from the initial state. This could explain a slightly faster early re-acquisition than early acquisition. Comparing the whole model output (net adaptation) and the experimental output, along both sessions, the model fitting was robust and highly significant (R^2=0.955). When fixing one state, thus using a single-state model, the fitting goodness decreased to R^2=0.8. It suggests that the two state multi-rate model could be generalized to VOR.

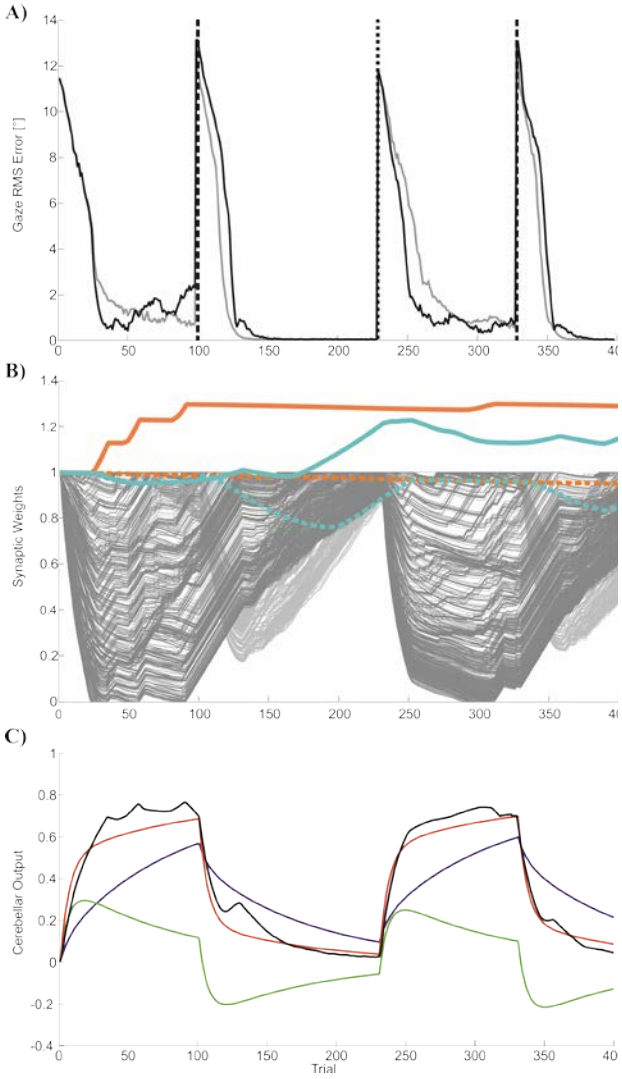

Figure 3. *Multiple-session VOR*

(A): the RMS gaze error along trials is reported; in grey when the eye motion was controlled by the 1-plasticity cerebellar model, in black by the 3-plasticity cerebellar model. The dashed vertical lines delimitate the acquisition and extinction phases of each session; *session1* and *session2* are separated by a vertical dotted line. (B): the synaptic weights at the three plasticity sites, for each trial. In grey: PF-PC (dark grey: on the "negative" PC; light grey: on the "positive" PC). In orange: MF-DCN (solid line: on the "negative" DCN; dashed line: on the "positive" DCN). In light blue: PC-DCN (solid line: on the "negative" DCN; dashed line: on the "positive" DCN). (C): the curves represent the cerebellar output, in terms of eye actuation signal: the model outputs (purple: slow state; green: fast state; red: net adaptation) and the real test output in black (RMS eye torque control signal within each trial) achieved with the 3-plasticity cerebellar controller, along the

IV. Discussion

In this robotic tests we have shown that a cerebellar controller with multisite plasticity can effectively drive a complex VOR paradigm in a real robot. The multisite plasticity proved superior to single-site plasticity in generating human-like VOR acquisition, extinction and

consolidation especially in complex tasks like gain-up and multi-session VOR.

These tests have allowed a functional role to be assigned to the multiple cerebellar plasticity sites. The 3-plasticity controller was able to behave both as timing and gain controller, demonstrating high accuracy in a closed-loop sensorimotor task. The cerebellar model extension with the DCN plasticity sites enhanced robot adaptation allowing to deal with changing stimuli and environmental conditions.

The underlying hypothesis is that the cerebellum learns on two different time-scales, so that the cerebellar cortex operates as a fast learning module while deeper structures, like the cerebellar nuclei, operate as a slow learning module [15]. The coexistence of two processes proceeding at different rates resembled EBCC learning in rabbits [15] and force-field learning in humans [19].

The existence of a fast rapidly reversible learning process emerged during the early acquisition and extinction phases. The existence of a slower process emerged in late acquisition. Moreover, the slow process could be associated to the consolidation mechanism evolving slowly along sessions.

In the model, the fast process was driven by large errors, while the slow process was driven by small errors. It is consistent with previous studies showing that in the vestibular-ocular reflex, inhibition of Purkinje cell activity affected only the adaptation mechanisms engaged by large errors [21].

Fast and slow processes were updated simultaneously from motor learning errors, supporting a parallel architecture of motor memory [13]. The direct association of the plasticity sites and the learning states was not straightforward: for example, DCN plastic changes were slower, but their effect was not exhaustively modeled by the slow state (a similar reasoning could be applied to cortical plasticity and the fast state). A deeper analyses, maybe using more states, could be needed to better model cerebellar learning.

V. CONCLUSIONS

In this work, for the first time, we have embedded a realistic cerebellar controller equipped with distributed plasticity into a neurorobot operating in real-time, challenging the system in the cerebellum-mediated closed-loop tasks The aim is to assess the role of multiple cerebellar plasticity in sensorimotor learning, thus fostering our understanding of human learning processes, linking low-level neural circuit mechanisms with high-level motor control and adaptation. As a further advance, the platform could be updated with new neurophysiological properties and the distributed plasticity model could be translated into a more realistic spike-timing computational scheme [22].

REFERENCES

[1] M. Ito, "Cerebellar control of the vestibulo-ocular reflex–around the flocculus hypothesis," *Annual review of neuroscience*, vol. 5, no. 1, pp. 275–297, 1982.

[2] M. Ito, "Cerebellar learning in the vestibulo-ocular reflex," *Trends in cognitive sciences*, vol. 2, no. 9, pp. 313–321, 1998.

[3] M. Ito, "Cerebellar microcomplexes," *International review of neurobiology*, vol. 41, pp. 475–487, 1997.

[4] N. F. Lepora, J. Porrill, C. H. Yeo, and P. Dean, "Sensory prediction or motor control? application of marr–albus type models of cerebellar function to classical conditioning," *Frontiers in computational neuroscience*, vol. 4, 2010.

[5] E. Franchi, E. Falotico, D. Zambrano, G. G. Muscolo, L. Marazzato, P. Dario, and C. Laschi, "A comparison between two bio-inspired adaptive models of vestibulo-ocular reflex (vor) implemented on the icub robot," in *Humanoid Robots (Humanoids), 2010 10th IEEE-RAS International Conference on*. IEEE, 2010, pp. 251–256.

[6] G. Cheron, B. Dan, and J. Márquez-Ruiz, "Translational approach to behavioral learning: Lessons from cerebellar plasticity," *Neural plasticity*, vol. 2013, 2013.

[7] J. L. McKinstry, G. M. Edelman, and J. L. Krichmar, "A cerebellar model for predictive motor control tested in a brain-based device," *Proceedings of the National Academy of Sciences of the United States of America*, vol. 103, no. 9, pp. 3387–3392, 2006.

[8] A. Lenz, S. R. Anderson, A. G. Pipe, C. Melhuish, P. Dean, and J. Porrill, "Cerebellar-inspired adaptive control of a robot eye actuated by pneumatic artificial muscles," *Systems, Man, and Cybernetics, Part B: Cybernetics, IEEE Transactions on*, vol. 39, no. 6, pp. 1420–1433, 2009.

[9] J. A. Garrido, N. R. Luque, E. D'Angelo, and E. Ros, "Distributed cerebellar plasticity implements adaptable gain control in a manipulation task: a closed-loop robotic simulation," *Frontiers in Neural Circuits*, vol. 7, 2013.

[10] C. Hansel, D. J. Linden, and E. D'Angelo, "Beyond parallel fiber ltd: the diversity of synaptic and non-synaptic plasticity in the cerebellum," *Nature neuroscience*, vol. 4, no. 5, pp. 467–475, 2001.

[11] Z. Gao, B. J. van Beugen, and C. I. De Zeeuw, "Distributed synergistic plasticity and cerebellar learning," *Nature Reviews Neuroscience*, vol. 13, no. 9, pp. 619–635, 2012.

[12] C. Burdess, "The vestibulo-ocular reflex: computation in the cerebellar flocculus," Ph.D. dissertation, Citeseer, 1996.

[13] J. Y. Lee and N. Schweighofer, "Dual adaptation supports a parallel architecture of motor memory," *The Journal of Neuroscience*, vol. 29, no. 33, pp. 10396–10404, 2009.

[14] R. Shadmehr, M. A. Smith, and J. W. Krakauer, "Error correction, sensory prediction, and adaptation in motor control," *Annual review of neuroscience*, vol. 33, pp. 89–108, 2010.

[15] J. F. Medina, K. S. Garcia, and M. D. Mauk, "A mechanism for savings in the cerebellum," *The Journal of Neuroscience*, vol. 21, no. 11, pp. 4081–4089, 2001.

[16] C. Casellato, J. Garrido, C. Franchin, G. Ferrigno, E. D'Angelo, and A. Pedrocchi, "Brain-inspired sensorimotor robotic platform learning in cerebellum-driven movement tasks through a cerebellar realistic model," *IJCCI 2013 - Proceedings of*

the 5th International Joint Conference on Computational Intelligence, pp. 568–573, 2013.

[17] E. D'Angelo, S. Solinas, J. Garrido, C. Casellato, A. Pedrocchi, J. Mapelli, D. Gandolfi, and F. Prestori, "Realistic modeling of neurons and networks: towards brain simulation," *Functional neurology*, vol. 28, no. 3, p. 153, 2013.

[18] N. Luque, J. Garrido, R. Carrillo, O.-M. Coenen, and E. Ros, "Cerebellarlike corrective model inference engine for manipulation tasks," *IEEE Transactions on Systems, Man, and Cybernetics, Part B: Cybernetics*, vol. 41, no. 5, pp. 1299–1312, 2011.

[19] M. A. Smith, A. Ghazizadeh, and R. Shadmehr, "Interacting adaptive processes with different timescales underlie short-term motor learning," *PLoS biology*, vol. 4, no. 6, p. e179, 2006.

[20] R. R. Kimpo, E. S. Boyden, A. Katoh, M. C. Ke, and J. L. Raymond, "Distinct patterns of stimulus generalization of increases and decreases in vor gain," *Journal of neurophysiology*, vol. 94, no. 5, pp. 3092–3100, 2005.

[21] E. S. Boyden, A. Katoh, and J. L. Raymond, "Cerebellum-dependent learning: the role of multiple plasticity mechanisms," *Neuroscience*, vol. 27, 2004.

[22] C. Casellato, A. Antonietti, J. Garrido, R. Carrillo, N. R. Luque, E. Ros, A. Pedrocchi, and E. D'Angelo, "A generalized model of learning: robotic control driven by a spiking cerebellar network," Submitted.